**Characterisation of amyloid oligomers by electrospray ionisation- ion mobility spectrometry-mass spectrometry**

Charlotte A. Scarff, Alison E. Ashcroft and Sheena E. Radford

Astbury Centre for Structural Molecular Biology, School of Molecular and Cellular Biology, University of Leeds, Leeds, LS2 9JT, UK.

Corresponding authors:

Alison E. Ashcroft, Astbury Centre for Structural Molecular Biology, School of Molecular and Cellular Biology, University of Leeds, Leeds, LS2 9JT, UK.

Tel. +44 113 343 7273

E-mail: a.e.ashcroft@leeds.ac.uk.

Sheena E. Radford, Astbury Centre for Structural Molecular Biology, School of Molecular and Cellular Biology, University of Leeds, Leeds, LS2 9JT, UK.

Tel. +44 113 343 3170

E-mail: s.e.radford@leeds.ac.uk.

Running head : Amyloid oligomer characterisation by ESI-IMS-MS

**Abstract**

Soluble oligomers formed during the self-assembly of amyloidogenic peptide and protein species are generally thought to be highly toxic. Consequently, thorough characterisation of these species is of much interest in the quest for effective therapeutics and for an enhanced understanding of amyloid fibrillation pathways. The structural characterisation of oligomeric species, however, is challenging as they are often transiently and lowly-populated, and highly heterogeneous. Electrospray ionisation-ion mobility spectrometry-mass spectrometry (ESI-IMS-MS) is a powerful technique which is able to detect individual ion species populated within a complex heterogeneous mixture and characterise them in terms of shape, stoichiometry, ligand binding capability and relative stability. Herein, we describe the use of ESI-IMS-MS to characterise the size and shape of oligomers of beta-2-microglobulin through use of data calibration and the derivation of models. This enables information about the range of oligomeric species populated *en route* to amyloid formation and the mode of oligomer growth to be obtained.

**Key Words:** Protein aggregation, amyloid, oligomerisation, native mass spectrometry, ion mobility spectrometry-mass spectrometry

Amyloid oligomer characterisation by ESI-IMS-MS

## 1. Introduction

The identification and characterisation of oligomers populated *en route* to amyloid fibril formation is a major challenge. In the early stages of protein aggregation multiple, rapidly-converting, transient and lowly-populated species are co-populated in solution, so the detection and characterisation of individual species is extremely difficult *(1)*. Mass spectrometry (MS) is one technique which lends itself to the study of such heterogeneous mixtures as it enables the detection of multiple ions within the same sample, at femtomolar concentrations, and their identification based on their mass-to-charge ratios (*m/z*). Nano-electrospray ionisation (nESI)-MS allows for the analysis of non-covalently bound species and there is good evidence to support the view that complexes observed in the gas phase are reflective of species populated in solution *(2-4)*. Ion mobility spectrometry (IMS)-MS, which separates ions based on their mobility through an inert gas under the influence of a weak electric field, allows ion species of the same *m/z* but different shapes to be separated such that the presence of different protein conformational states and oligomeric species can be distinguished confidently *(5,6)*. Oligomer formation can be followed over time and any changes in oligomer distribution or protein conformation can be monitored *(7)*. Potential small molecule inhibitors can also be added to the protein and binding to specific protein conformers or oligomers detected *(8,9)*. Ion mobility measurements obtained on the Synapt HDMS travelling-wave ESI-IMS-MS instrument *(10)*, as used herein, can be converted by use of a suitable calibration to estimated rotationally-averaged collision cross-sections (CCSs) for individual ion species *(11-13)*. These can then be compared with modelled structures of monomers and/or oligomers and insights into the mechanism of oligomeric growth obtained *(14)*. Traditional drift tube IMS-MS instruments can also be used for analyses of this type and measurements obtained on these instruments can be directly converted to CCSs *(15)*. ESI-IMS-MS can also be used to study the relative stability of individual ion species by accelerating these species through the instrument under different voltages and recording their unfolding and dissociation profiles *(16)*. Additionally, subunit dynamics can be studied by mixing isotopically-labelled species

3

Amyloid oligomer characterisation by ESI-IMS-MS

with non-labelled species (e.g. [15]N and ^{14}N labelled proteins) and analysing the rate of subunit exchange in real time *(5,17)*.

Here ESI-IMS-MS is applied to the study of oligomers of a variant of beta-2-microglobulin (β2m) named ΔN6, a truncated variant without the first six N-terminal residues, which undergoes aggregation at neutral pH into amyloid fibrils *(18,19)*. β2m is the causative agent of dialysis-related amyloidosis and both wild-type b2m and ΔN6 have been found in amyloid plaques *(20)*. Ion mobility measurements obtained are calibrated by use of protein calibrants (with known CCSs) to produce estimated CCSs for each ion species. Estimated CCSs are compared with those obtained from model structures to allow for an understanding of the mechanism of oligomer growth.

## 2. Materials

### 2.1 Samples for ESI-IMS-MS analysis

1. Caesium iodide
2. Beta-2-microglobulin variant ΔN6
3. Cytochrome c
4. Bovine serum albumin (BSA)
5. Concanavalin A
6. Alcohol dehydrogenase (ADH)

### 2.2 Solvents and chemicals for ESI-IMS-MS analysis

1. Isopropanol (HPLC grade)
2. Water (HPLC grade)
3. Ammonium acetate

4.  Ammonium bicarbonate

5.  Desalting columns or buffer-exchange devices

6.  Gold/palladium-coated nanoflow needles

7.  GELoader tips (Eppendorf)

### 2.3 Mass Spectrometry Instrumentation and Data Acquisition, Analysis and Interpretation

1. Synapt HDMS Instrument equipped with a nanoflow ESI source and needle holder (Waters Corporation)

2. MassLynx 4.1with Driftscope (Waters Corporation)

3. MOBCAL software (http://www.indiana.edu/~nano/software.html)

4. FORTRAN compiler and editor

5. TextPad

## 3. Methods

### 3.1 Sample preparation

For the study of protein oligomers by ESI-MS, solution conditions must be found not only in which the protein undergoes the aggregation process of interest on a suitable time scale but also that are MS-compatible (see Note 1). Most buffers used for *in vitro* biochemical experiments, such as Tris.HCl and MOPS, are incompatible with ESI-MS analysis as they are largely non-volatile, resulting in suppression of ionisation and/or extensive adduct formation *(21)*. Proteins purified or stored in these types of buffers can be buffer-exchanged to allow for ESI-MS analysis by use of buffer exchange devices or desalting columns (see Note 2). Adequate removal of non-volatile buffer components is often the most critical parameter governing spectral quality and so buffer-exchange must be stringent. Typically, proteins are buffer-exchanged into aqueous volatile buffer solutions such as ammonium acetate, ammonium formate or ammonium bicarbonate solution. The choice of buffer will be dependent on the protein and aggregation properties under study and the desired ionic strength and pH

5

Amyloid oligomer characterisation by ESI-IMS-MS

(see Notes 3 and 4). If buffer additives such as metal ions, cofactors or reducing agents, are required to maintain protein stability or to maintain aggregation properties these can be added up to approximately 1 mM concentration without significantly influencing spectral quality *(21)*.

For the study of aggregation of ΔN6 at pH 6.2 the following sample preparation procedure was undertaken:

1. Lyophilised ΔN6 (1-2 mg) was resuspended in buffer A (50 mM ammonium bicarbonate, 120 mM ammonium acetate solution pH 6.2) to a final volume of 1 mL.
2. 100 µL was desalted by use of a Zeba™ Spin Desalting Column (7K MWCO, ThermoFisher Scientific) equilibrated with buffer A.
3. The concentration of the protein solution was determined by measurement of the absorbance at 280 nm using a molar extinction coefficient 20065 $M^{-1}$ $cm^{-1}$. The sample was diluted to a working concentration of 40 µM.
4. Protein calibrants, cytochrome c, BSA, concanavalin A and ADH, were prepared in 200 mM ammonium acetate solution to a working concentration of 10-20 µM following desalting by use of Zeba™ Spin Desalting Columns.
5. CsI solution, for mass calibration, was prepared by dissolving in 50 % (v/v) water/ isopropanol to a concentration of 2 mg/mL (Note 5).

*3.2 ESI-IMS-MS analysis*

ESI-IMS-MS analysis was performed on a Synapt HDMS instrument, which has a quadrupole/ travelling-wave ion mobility (TWIM)/ orthogonal time-of-flight geometry. The instrument is equipped with a nESI source and a 32,000 *m/z* range RF generator. nESI allows for the analysis of small sample volumes, enhanced desolvation efficiency of protein molecules from droplets, improved sensitivity and increased tolerance to buffer salts in comparison to conventional ESI *(21)*.

Samples were introduced into the instrument by the use of in-house prepared capillaries. These are borosilicate glass-capillaries with a tapered edge coated with a mixture of gold and palladium. Capillaries were prepared by use of a micropipette puller (Model P-97, Sutter Instrument Co.) and coated using a sputter coater with a gold/palladium target (Emitech Sc7620). The puller must be programmed to produce capillary tips with acceptable shapes and this is a trial-and-error process *(21)*. The diameter of the capillaries is critical to be able to obtain a stable spray and requires optimisation. Capillary tips often need to be trimmed to obtain the ideal length and orifice diameter for spraying. This is sample dependent and again a trial-and-error process. Capillaries can also be purchased from various sources, such as Waters Corporation and Proxeon Biosystems, but may not yield the same spray properties as those prepared in-house.

For the acquisition of ESI-IMS-MS data of ΔN6 oligomeric species:

1. CsI solution was used for tuning and mass calibration of the instrument.
2. ΔN6 was analysed under various instrument parameters and optimal instrument conditions for analysis obtained (discussed in further detail below).
3. Data were acquired under optimised conditions at three different wave heights to allow for CCS calibration.

The optimal parameters for the study of oligomeric species may not be the same as for the study of monomeric species and so data often need to be obtained under various instrument parameters and compared and contrasted. Instrument parameters of particular importance to data acquisition are listed in Table 1 and discussed in more detail below. Further discussion of instrument parameters for the study of non-covalent complexes in general can be found elsewhere *(11,21)*.

A key parameter to optimise for the efficient transfer of non-covalent oligomers into the mass spectrometer is the backing pressure in the source region of the instrument. Increasing the backing

pressure results in collisional cooling of the ions and therefore aids in the transmission of ions with high *m/z* *(22)*. The backing pressure can be altered by partially closing the Speedivalve (isolation valve) for the roughing pump and therefore changing the conductance of the source vacuum line *(21)*.

Another important parameter that requires optimisation is the cone voltage. Figure 1 shows spectra of ΔN6 obtained under two different cone voltages (Figures 1a and 1b). At a higher cone voltage (170 V) spectral quality is improved significantly due to increased desolvation of protein species, resulting in an increased signal-to-noise ratio and increased mass accuracy, thus allowing for confident assignments of ion species based on their *m/z*. However, use of a higher cone voltage can lead to gas-phase unfolding (as determined by ion mobility) and charge stripping of some ion species (Figures 1c-e). Figures 1c and 1d show driftscope plots corresponding to the spectra shown in Figures 1a and 1b respectively and Figure 1e shows extracted arrival time distributions (ATDs) for ions with *m/z* 2784. The driftscope plots show drift time on the x axis, *m/z* on the y axis and relative ion intensity on the z axis. Gas-phase activation and unfolding of the ion species monomer (4+), dimer (8+) and trimer (12+) occurs at the higher cone voltage (170 V) that is not observed at the lower cone voltage (30 V) (Figures 1c and 1d, inset dashed box and Figure 1e) yet the dimeric ion species (5+) at the higher *m/z* 4455 is unaffected by this increased voltage (Figures 1c and 1d, inset dotted box). The instrument parameters that yield the highest quality mass spectra in terms of signal-to-noise and mass accuracy are therefore not those that best preserve solution-phase properties. Acquisition of data under both of these contrasting instrument conditions, however, allows peaks to be accurately assigned and ion mobility measurements to be performed on gas-phase structures that are most likely to be reflective of those present in solution.

One of the advantages of the use of ion mobility coupled with MS is that multiple oligomeric species present at the same *m/z* value can be separated, identified and characterised in terms of their shape (as illustrated in Figure 1e). Ion mobility separation depends on mass, charge and shape of an ion species.

Ions with a more compact structure will experience fewer collisions with the buffer gas in comparison to ions with a more extended structure and thus will exit the ion mobility cell faster. Ions with higher charges will also traverse the drift cell faster so higher-order oligomeric species will normally have shorter drift times than lower-order oligomeric species present at the same *m/z*. This, however, is not always the case and so carbon isotope distributions and the *m/z* spacing of sodiated peaks can aid in the determination of oligomer number from arrival time distributions. For *m/z* 2784, three peaks are observed in the ATD (170 V) (shown in Figure 1e) centred approximately at drift times of 10, 11 and 12 ms respectively. Extraction of the mass spectrum for the last peak (centred at 12 ms) results in a *m/z* 2784 species with a carbon isotope spacing of 0.25, indicating that this ion possesses four charges and hence has a molecular mass of approximately 11.1 kDa and therefore corresponds to a monomeric species (i.e. $M^{4+}$) (Figure 1f, lower panel). Extraction of the mass spectrum for the peak centred at 11 ms indicates that this ion is more highly-charged as the isotope spacing is not discernible ($D^{8+}$) (Figure 1f, upper panel). It is also interesting to note that within the mass spectrum the centroid mass shifts to the right between the monomeric and dimeric ion (Figure 1f). This is because for the monomeric ion species the monoisotopic peak is visible but for the dimer the monoisotopic peak is no longer observable as the percentage of species that contain only $C^{12}$ atoms is negligible.

Optimisation of ion mobility parameters is of great importance to obtain good separation of ion species. Three travelling wave ion guides (TWIGs), the trap, ion mobility cell and transfer region, form the TWIM device *(10,23)*. The trap periodically gates a packet of ions into the ion mobility cell. This packet of ions is then separated on account of the different mobilities of the ions, with the time it takes each ion to traverse the mobility cell and reach the TOF pusher recorded. For each gated pulse, 200 orthogonal acceleration pushes of the TOF pusher are recorded to form one ion mobility experiment. The drift time of an ion species is therefore proportional to the pusher frequency, which is dependent on *m/z* acquisition range. Figure 2 shows the total ion chromatograms obtained upon analysis of ΔN6 under three different sets of ion mobility conditions over the 500-8000 *m/z* mass range. At 300 m/s wave velocity (WV) and 7 V wave height (WH) little separation of ion species is

obtained. Much better separation of ion species is obtained by use of a ramped WH from 5-15 V. At 400 m/s WV, 7 V WH not all ion species have exited the ion mobility cell and reached the TOF pusher before the next set of ions have been pulsed into the ion mobility cell, this is termed rollover. Rollover is evident when the total ion chromatogram does not reach baseline intensity within one ion mobility experiment (0-25.5 ms in this example). Accurate drift times for individual ion species cannot be determined unless all ions are contained within the same mobility pulse.

For the optimisation of instrument parameters for the acquisition of spectra of ΔN6 oligomeric species the following steps were taken:

1. Approximately 10 µL of sample solution was loaded into a capillary using a GELoader tip and the end of the capillary was positioned perpendicular to the MS sample cone.

2. The position of the capillary relative to the sampling cone and the length of the capillary tip were optimised. A stable spray from the nanoflow capillary was obtained at the lowest capillary voltage possible (Note 6).

3. The backing pressure of the mass spectrometer was increased in 0.5 mBar steps until the largest population of higher-order oligomeric species could be seen (this was conducted at both high and low cone voltages so influence of cone voltage on the quality of the resulting spectra could be considered).

4. Extraction cone, trap collision energy and transfer collision energy were optimised at low cone voltage to achieve the greatest ion transmission without inducing gas-phase unfolding or dissociation.

5. Ion mobility parameters were optimised to provide the greatest separation of ion species without rollover by use of a ramped wave height (Figure 2, 5-15V) and spectra were recorded at both low and high cone voltages (30-170 V).

6. The wave height was changed from a ramped to a fixed value and spectra acquired under low and high cone voltage conditions at three fixed wave heights that provided ion mobility separation without rollover.

### 3.3 ESI-IMS-MS data calibration

Drift time measurements obtained from ESI-IMS-MS analysis can be used to provide estimates of the CCS of an ion species, which can then be compared with values obtained from atomic resolution structures or estimated values from model structures *(12,14)*. On the Synapt ESI-IMS-MS instrument, a direct conversion between drift time and CCS is not possible and so CCS measurements may be estimated by use of a calibration obtained by analysis of protein standards with known CCSs obtained from drift tube ion mobility measurements.

Several choices of calibrants are available and the most appropriate for each analyte of interest must be chosen. Clemmer provides a database of cross-section measurements for denatured proteins (cytochrome c, ubiquitin, lysozyme) and peptides (tryptic digests of ADH and cytochrome c) (http://www.indiana.edu/~clemmer/Research/Cross%20Section%20Database/cs_database.php) whilst Bush *et al.* provide measurements obtained for proteins analysed under native conditions, ranging from cytochrome c at 12 kDa with a cross-section of 1490 $Å^2$ (in $N_2$) to GroEL at 801 kDa and a CCS of approximately 21800 $Å^2$ (in $N_2$) *(24)*.

The calibration standards used must be analysed under identical instrument conditions for all parameters downstream of the trapping ion guide as used for the protein of interest *(11)*. Ideally, the same class of molecules should be used for calibration as that of the sample of interest i.e. native protein calibrants used to calibrate data obtained for a protein of interest under native solution conditions and peptide calibrants for peptide data. Due to the nature of the ion mobility separation and the relationship between drift time and CCS, in order to obtain accurate CCSs ion mobility measurements must be made under fixed wave heights and not by use of a wave height ramp. The

corrected arrival times of the calibration standards must also bracket those of the analyte for the calibration to be valid *(25)*.

To perform the calibration the following steps are undertaken:

1. The modal arrival time $(t_d)$ at which each calibrant ion arrives at the detector is extracted from the ion mobility data (Note 7).

2. The arrival time is corrected for *m/z* dependent flight time. The *m/z* dependent flight time is proportional to the square root of the *m/z*. It must be subtracted to obtain the corrected effective drift time $(t'_d)$, i.e. the time taken to traverse the mobility cell. The corrected effective drift time $(t'_d)$ is given by:

$$t'_d = t_d - \frac{c\sqrt{m/z}}{1000}$$

where c is the enhanced duty cycle (EDC) delay coefficient found in the instrument settings (Note 8).

3. Calibration coefficients are obtained from published absolute cross-section data $(\sigma)$. Published cross-sections are corrected to take into account the effects of reduced mass and charge state. Where $e$ is the charge on the ion, $m_i$ is the mass of the ion and $m_n$ is the mass of the mobility gas, normalised cross-sections $(\sigma')$ are given by:

$$\sigma' = \frac{\sigma}{e \times \sqrt{\left(\frac{1}{m_i} + \frac{1}{m_n}\right)}}$$

4. $\sigma'$ is plotted against $t'_d$.

A power series fit ($y = Ax^B$) or a linear series fit ($y = Ax + B$) to the data points is applied. A power series fit has been shown to provide a more reliable calibration for large compounds, such as proteins, whereas a linear relationship has been found to be more appropriate for smaller molecules, such as peptides *(26)*. For denatured calibrants an $r^2$ fit should be $>0.98$ and for native calibrants $>0.95$ for the calibration to be acceptable.

5. Experimental T-Wave mobility measurements obtained for an analyte are converted into estimated CCSs by correction for reduced mass and charge and application of the power series fit or the linear series fit as appropriate.

$$CCS = A \times {t'_d}^B \times e \times \sqrt{\left(\frac{1}{m_i} \times \frac{1}{m_n}\right)}$$

or

$$CCS = [(A \times t'_d) + B] \times e \times \sqrt{\left(\frac{1}{m_i} \times \frac{1}{m_n}\right)}$$

Plotting estimated CCS against charge state for individual oligomeric species can be used to help ensure the correct assignments have been made. CCS should increase with an increase in charge state and if this is not the case it is likely that an incorrect assignment has been made.

For the calculation of CCSs for ΔN6 oligomeric species the following steps were undertaken:

1. Data were acquired for the calibrants cytochrome c, BSA, concanavalin A and ADH under the optimised instrument conditions (from the trap onwards with low cone voltage) used for analysis of ΔN6 (at fixed wave heights).

2. Modal drift times for each calibrant ion were extracted from ATDs and used to produce a calibration with a power fit following the procedure detailed above for each wave height. A typical calibration is shown in Figure 3.

3. Modal drift times for each ΔN6 species were extracted from their ATDs and their CCSs calculated by use of the appropriate calibration.

4. Average CCS measurements for each oligomeric species and each charge state were calculated by averaging measurements obtained from three replicate experiments. The error in the calibration measurement is usually in the range of 5-8 % (Note 9) *(11)*.

### *3.4 Modelling*

CCS values estimated from ion mobility data can be compared to calculated CCS values from available high-resolution structures or coarse-grain models. This can allow for comparison of CCS measurements obtained in the gas phase to solution-phase measurements. CCS values calculated for atomic structures are generally in good agreement with those calculated by IMS. The lowest charged ion species are generally thought to be most reflective of solution-phase structure and so measurements are most often compared to these.

Calculation of CCS values from atomic structures or coarse-grain models can be performed by the use of MOBCAL. MOBCAL, an open source program to calculate mobilities *(27,28)*, facilitates the use of three approximations to calculate CCSs. The simplest method is the projection approximation (PA). This replaces the CCS of an ion with its projection (shadow) and averages the projections created by every orientation of that ion *(29)*. The PA is an adequate approximation for small molecules but tends to underestimate the CCS of protein ions with highly convex structures where buffer gas interactions

become important *(28)*. The trajectory method (TM) gives the most reliable estimate, incorporating all interactions but is computationally intense (taking in excess of a week to calculate the CCS from an atomic structure for a 10 kDa protein on a single processor). A compromise is to use a third model, the exact hard sphere scattering (EHSS) method. This ignores electrostatic interactions so requires substantially less computational time, and can calculate CCSs to within a few percent of values obtained by the trajectory method *(28)*. More recently, the Bowers and Bleiholder groups have developed the projected superposition approximation (PSA) method to calculate CCSs from structures (http://luschka.bic.ucsb.edu:8080/WebPSA/) *(30-33)*. This is a more accurate version of the PA that takes into account a shape factor and so has been shown to provide more reliable estimates of CCS than the PA or EHSS approach but in significantly less time than required to run the TM.

For coarse grain modelling of oligomer structures, isotropic and linear growth can be estimated by the use of equations. In isotropic growth, $\sigma_n = \sigma_m * n^{2/3}$, where n = oligomer number, $\sigma_n$ is the CCS of oligomer number n and $\sigma_m$ is the CCS of the monomer *(14)*. Similarly, linear growth in one direction (fibril growth) can be estimated by $\sigma_n = a * n + k$, where a describes the CCS of a monomer within a fibril and k is the size of the fibril cap. For more complex models of oligomer growth, spheres representative of the shape and size of a single subunit (monomer) within an oligomer can be arranged in three-dimensional space to build models. A CCS for these more complex models can be calculated by use of the MOBCAL software and the PA method. The mass and radius of a single monomer subunit is required along with the x,y,z coordinates of each monomer centre contained within the model.

Here, isotropic and linear growth pathways of ΔN6 oligomers were modelled by use of the equations given above and MOBCAL was used to produce a ring model of oligomeric growth. For the linear growth model, estimated monomeric and dimeric CCSs (for the lowest charge states of each species observed) from ion mobility data were used to determine a and k by solving the two simultaneous

equations $\sigma_1 = a*1 + k$ and $\sigma_2 = a*2 + k$. To use MOBCAL to calculate CCSs, input files for MOBCAL need to be generated (.mfj) and the MOBCAL code needs to be modified. Force 3.0 (free distribution software) was used to compile and edit the FORTRAN script and input files were generated in TextPad. The input file needs to be in a specific format and contain the Cartesian coordinates of each atom or monomer within the model structure. Further description of the layout of .mfj files is given below and can be found in the "read me" information provided with the MOBCAL script at (http://www.indiana.edu/~nano/software.html).

For calculation of the ring model of oligomeric growth by use of MOBCAL the following steps were undertaken:

1. The MOBCAL script was edited by use of the FORTRAN editor and compiler Force 3.0 in two sections of the code that define atom mass and radii (lines ~ 580 and ~2600). Atom mass and atom radius were replaced with ΔN6 monomer mass and ΔN6 monomer radius. The radius of the ΔN6 monomer was calculated based on a spherical particle that would give rise to the monomeric CCS estimated by ESI-IMS-MS ($\pi r^2$). The script was also edited to stop calculation of the TM by placing a c in front of line 338 *(11)*.

2. Coordinate entry .mfj files for the MOBCAL script were generated in TextPad with the following structure:

    Line 1: name of model

    Line 2: number of models (always 1 in this case)

    Line 3: number of monomers in model

    Line 4: ang

    Line 5: none

    Line 6: 1.0000

    Line 7: x,y and z coordinate of first atom (monomer), followed by monomer mass separated by indents.

Line 7+n: x,y and z coordinate of (first +n) atom (monomer), followed by

monomer mass separated by indents.

Line 7+n+1:  number of monomers in model


e.g.

ΔN6__DIMER

1

2

ang

1.0000

    1.000   1.000   1.000   11136

    1.000   1.000   25.00   11136

2


3.  The script was compiled and executed using Force 3.0. and the mobcal.run file was edited so it used the generated .mfj file as input.

4.  The appropriate spacing between two monomer centres to use within the models was determined by varying the distance between two monomers in the model for the dimer until the script successfully calculated the estimated dimeric CCS. All models generated in this way use the monomeric and dimeric CCSs estimated from ion mobility data to instruct higher-order oligomer models.

5.  Coordinate .mfj files for higher-order oligomers were generated by use of trigonometry to determine the x,y,z coordinates for the centre of each monomer within the model of a trimer, tetramer and pentamer *en route* to a regular hexagon structure.

Figure 4 shows the CCS values estimated from IMS-MS experiments for the lowest charge states of each oligomer of ΔN6 observed alongside CCS values calculated for various models of oligomer growth. Estimated CCSs for oligomers of ΔN6 are larger than expected for an isotropic mode of oligomer growth yet smaller than expected for both the linear and ring models of oligomeric growth. These simple models are thus insufficient to describe the oligomer formation pathway for ΔN6. More complex assembly mechanisms or a switch in mechanism with oligomer size are thus needed to describe the experimental data.

## 4. Notes

1. Simply replacing a non-volatile buffer with a volatile buffer at the same pH and ionic strength may not yield the same aggregation parameters. The rate and mechanism of aggregation may depend on ion composition as well as ionic strength and pH. The aggregation process must therefore be analysed by other biophysical techniques such as fluorescence, turbidity, analytical ultracentrifugation and/or electron microscopy to ensure that the protein aggregation pathway followed is comparable between two different buffer systems (see references 1,5 and 7 for further details).

2. Buffer exchange can be performed using desalting columns or buffer exchange devices, such as Zeba™ Spin Desalting Columns (7K MWCO, ThermoFisher Scientific) or Micro Bio-Spin 6 chromatography columns (6K MWCO, Bio-Rad). Dialysis may also be used but may not be a suitable approach if the protein of interest aggregates on a short time scale at low temperature as aggregation will proceed during the time taken to perform the dialysis. If a protein sample is already at a low concentration it can be buffer-exchanged and concentrated by use of centrifugal devices, such as Ultrafree-0.5 and Microcon (Millipore), or Vivaspin 500 µL concentrators (Millipore).

3. Buffer salt concentrations from 10 mM to 1M are routinely used, with higher concentrations reducing the negative effects of any remaining non-volatile buffer components *(21)*.

4. Due to the pKa values of acetate and bicarbonate it is difficult to buffer a solution between pH 6 and 8, which is the physiological pH range experienced by most proteins. A mixture of ammonium bicarbonate and ammonium acetate solutions can be used to try and achieve this. Many studies, however, use ammonium acetate solutions at pH 7, which do not buffer well at this pH. In this case, care must be taken to ensure that the pH of the solution is not changing during aggregation as this may influence the nature of aggregates formed and the aggregation pathway followed.

5. The concentration of CsI used can be increased in order to cover a wider *m/z* calibration range.

6. Experience has shown that the minimum capillary voltage required to generate a stable spray generally produces the optimum MS-spectrum *(34)*.

7. The extracted ATD for each calibrant ion may have multiple features, suggesting multiple conformations of the calibrant ion are present. Multiple σ's for a given charge state are published for some calibrant species but not for all. For calibrant ions, for which only a single σ is published the most abundant feature in the ATD, which usually has the shortest drift time of the all the features, is usually chosen for calibration purposes. A calibration with a low correlation coefficient may result if an incorrect feature in the ATD for a calibrant ion is used.

8. The EDC value is constant provided that the parameters for the transfer T-Wave guide and the transfer ion optics remain unchanged since EDC calibration *(11)*.

9. The error in the CCS measurements can be estimated by the sum of the reproducibility (standard deviation of three or more replicate measurements), the average error of the calibration curve ($< 2.5$ %) and the error in measurement of the protein standards used to produce the calibration (assumed to be 1 %) *(11)*.

## Acknowledgements

## References

1. Woods LA, Radford SE, Ashcroft AE (2013) Advances in ion mobility spectrometry–mass spectrometry reveal key insights into amyloid assembly. *Biochim Biophys Acta Proteins* 1834,1257-1268

2. Hilton GR, Benesch JLP (2012) Two decades of studying non-covalent biomolecular assemblies by means of electrospray ionization mass spectrometry. *J R Soc Interface* 9,801-816

3. Ruotolo BT, Robinson CV (2006) Aspects of native proteins are retained in vacuum. *Curr Opin Chem Biol* 10,402-408

4. Ruotolo BT, Giles K, Campuzano I et al. (2005) Evidence for macromolecular protein rings in the absence of bulk water. *Science* 310,1658-1661

5. Smith DP, Radford SE, Ashcroft AE (2010) Elongated oligomers in β2-microglobulin amyloid assembly revealed by ion mobility spectrometry-mass spectrometry. *Proc Natl Acad Sci USA* 107,6794-6798

6. Smith DP, Giles K, Bateman RH et al. (2007) Monitoring copopulated conformational states during protein folding events using electrospray ionization-ion mobility spectrometry-mass spectrometry. *J Am Soc Mass Spectrom* 18,2180-2190

7. Smith DP, Woods LA, Radford SE et al. (2011) Structure and dynamics of oligomeric intermediates in β2-microglobulin self-assembly. *Biophys J* 101,1238-1247

8.      Woods LA, Platt GW, Hellewell AL et al. (2011) Ligand binding to distinct states diverts aggregation of an amyloid-forming protein. *Nat Chem Biol* 7,730-739

9.      Young LM, Cao P, Raleigh DP et al. (2013) Ion mobility spectrometry–mass spectrometry defines the oligomeric intermediates in amylin amyloid formation and the mode of action of inhibitors. *J Am Chem Soc* 136,660-670

10.     Pringle SD, Giles K, Wildgoose JL et al. (2007) An investigation of the mobility separation of some peptide and protein ions using a new hybrid quadrupole/travelling wave ims/oa-tof instrument. *Int J Mass Spectrom* 261,1-12

11.     Ruotolo BT, Benesch JLP, Sandercock AM et al. (2008) Ion mobility-mass spectrometry analysis of large protein complexes. *Nat Protoc* 3,1139-1152

12.     Scarff CA, Thalassinos K, Hilton GR et al. (2008) Travelling wave ion mobility mass spectrometry studies of protein structure: Biological significance and comparison with x-ray crystallography and nuclear magnetic resonance spectroscopy measurements. *Rapid Commun Mass Spectrom* 22,3297-3304

13.     Smith DP, Knapman TW, Campuzano I et al. (2009) Deciphering drift time measurements from travelling wave ion mobility spectrometry-mass spectrometry studies. *Eur J Mass Spectrom* 15,113-130

14.     Bleiholder C, Dupuis NF, Wyttenbach T et al. (2011) Ion mobility–mass spectrometry reveals a conformational conversion from random assembly to β-sheet in amyloid fibril formation. *Nat Chem* 3,172-177

15.     Lanucara F, Holman SW, Gray CJ et al. (2014) The power of ion mobility-mass spectrometry for structural characterization and the study of conformational dynamics. *Nat Chem* 6,281-294

16.     Zhong Y, Han L, Ruotolo BT (2014) Collisional and coulombic unfolding of gas-phase proteins: High correlation to their domain structures in solution. *Angew Chem Int Ed Engl*, doi: 10.1002/anie.201403784

17.     Leney AC, Pashley CL, Scarff CA et al. (2014) Insights into the role of the beta-2 microglobulin d-strand in amyloid propensity revealed by mass spectrometry. *Mol Biosyst* 10,412-420

18.     Eichner T, Kalverda AP, Thompson GS et al. (2011) Conformational conversion during amyloid formation at atomic resolution. *Mol Cell* 41,161-172

19.     Sarell CJ, Woods LA, Su Y et al. (2013) Expanding the repertoire of amyloid polymorphs by co-polymerization of related protein precursors. *J Biol Chem* 288,7327-7337

20.     Bellotti V, Stoppini M, Mangione P et al. (1998) β2-microglobulin can be refolded into a native state from ex vivo amyloid fibrils. *Eur J Biochem* 258,61-67

21.     Hernandez H, Robinson CV (2007) Determining the stoichiometry and interactions of macromolecular assemblies from mass spectrometry. *Nat Protoc* 2,715-726

22.     Chernushevich IV, Thomson BA (2004) Collisional cooling of large ions in electrospray mass spectrometry. *Anal Chem* 76,1754-1760

23.     Giles K, Pringle SD, Worthington KR et al. (2004) Applications of a travelling wave-based radio-frequencyonly stacked ring ion guide. *Rapid Commun Mass Spectrom* 18,2401-2414

24.     Bush MF, Hall Z, Giles K et al. (2010) Collision cross sections of proteins and their complexes: A calibration framework and database for gas-phase structural biology. *Anal Chem* 82,9557-9565

25.     Shvartsburg AA, Smith RD (2008) Fundamentals of traveling wave ion mobility spectrometry. *Anal Chem* 80,9689-9699

26.     Thalassinos K, Grabenauer M, Slade SE et al. (2009) Characterization of phosphorylated peptides using traveling wave-based and drift cell ion mobility mass spectrometry. *Anal Chem* 81,248-254

27.     Shvartsburg AA, Jarrold MF (1996) An exact hard-spheres scattering model for the mobilities of polyatomic ions. *Chem Phys Lett* 261,86-91

28.     Jarrold MF (1999) Unfolding, refolding, and hydration of proteins in the gas phase. *Acc Chem Res* 32,360-367

29.     Mack E (1925) Average cross-sectional areas of molecules by gaseous diffusion measurements. *J Am Chem Soc* 47,2468-2482

30.     Bleiholder C, Wyttenbach T, Bowers MT (2011) A novel projection approximation algorithm for the fast and accurate computation of molecular collision cross sections (i). Method. *Int J Mass Spectrom* 308,1-10

31.     Bleiholder C, Contreras S, Do TD et al. (2013) A novel projection approximation algorithm for the fast and accurate computation of molecular collision cross sections (ii). Model parameterization and definition of empirical shape factors for proteins. *Int J Mass Spectrom* 345–347,89-96

32.     Bleiholder C, Contreras S, Bowers MT (2013) A novel projection approximation algorithm for the fast and accurate computation of molecular collision cross sections (iv). Application to polypeptides. *Int J Mass Spectrom* 354–355,275-280

33.     Anderson SE, Bleiholder C, Brocker ER et al. (2012) A novel projection approximation algorithm for the fast and accurate computation of molecular collision cross sections (iii): Application to supramolecular coordination-driven assemblies with complex shapes. *Int J Mass Spectrom* 330–332,78-84

34.     Campuzano I, Giles K (2011) Nanospray ion mobility mass spectrometry of selected high mass species. In: Toms SA, Weil RJ (eds) Nanoproteomics, vol 790. Methods in molecular biology. Humana Press, pp 57-70. doi:10.1007/978-1-61779-319-6_5

**Figure Captions**

Figure 1. Mass spectra of ΔN6 (40 µM) in 50 mM ammonium bicarbonate 120 mM ammonium acetate pH 6.2 obtained at a cone voltage of (**a**) 30 V and (**b**) 170 V with inset *m/z* region 3950-4400 magnified, M = monomer, D = dimer, T = trimer, Q = tetramer, P = pentamer; (**c**) and (**d**) corresponding ESI-IMS-MS driftscope plots respectively with *m/z* 2784 highlighted in dashed boxes; (**e**) extracted arrival time distributions for *m/z* 2784 at 30 V and 170 V cone voltage; (**f**) mass spectra corresponding to $M^{4+}$ and $D^{8+}$ extracted from arrival time distribution peaks labelled in (**e**).

Figure 2. Total ion chromatograms obtained upon the ESI-IMS-MS analysis of ΔN6 under different ion mobility conditions: (**a**) wave velocity (WV) 300 m/s wave height (WH) 7 V; (**b**) WV 300 m/s ramped WH 5-15 V; (**c**) WV 400 m/s WH 7 V.

Figure 3. Ion mobility data calibration with absolute CCSs corrected for reduced mass and charge ($\sigma'$) for cytochrome c (open diamonds), BSA (filled diamonds), concanavalin A (open squares) and ADH (filled squares) plotted against corrected drift times ($t'_d$) for calibrant ions. A power series fit is shown.
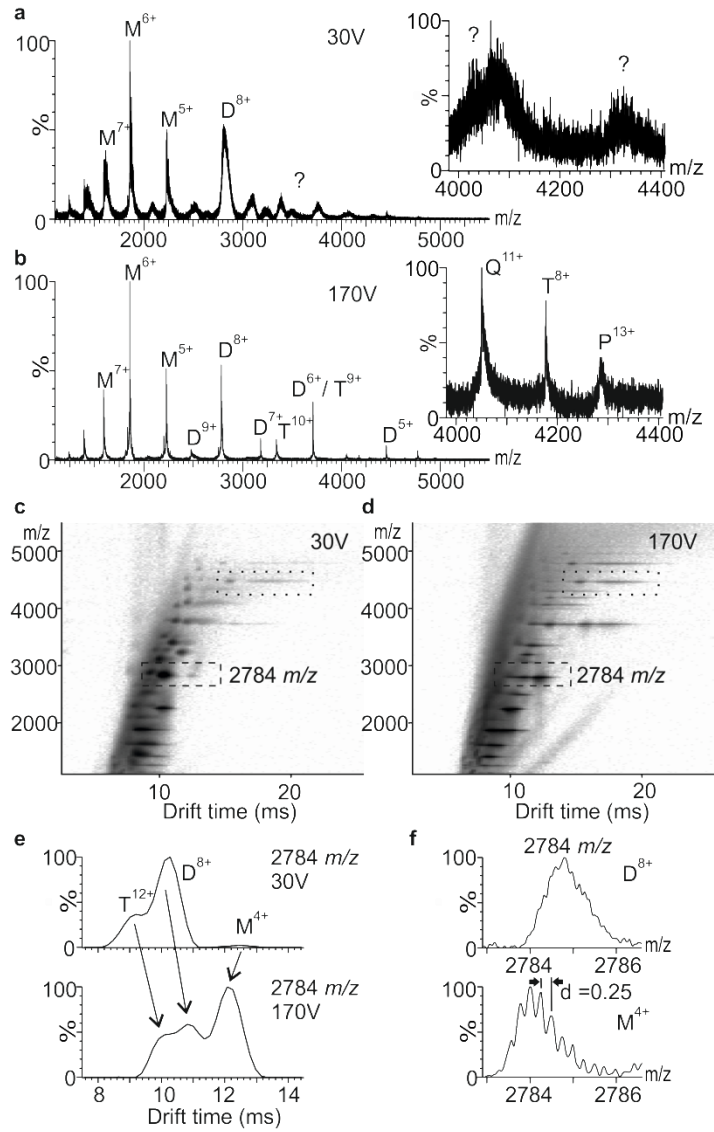
Figure 4. Estimated CCS values for ΔN6 oligomers of different oligomer number (n) (filled diamonds). Various models of oligomer growth are shown: isotropic (solid line); ring (dashed line); linear (dotted line).
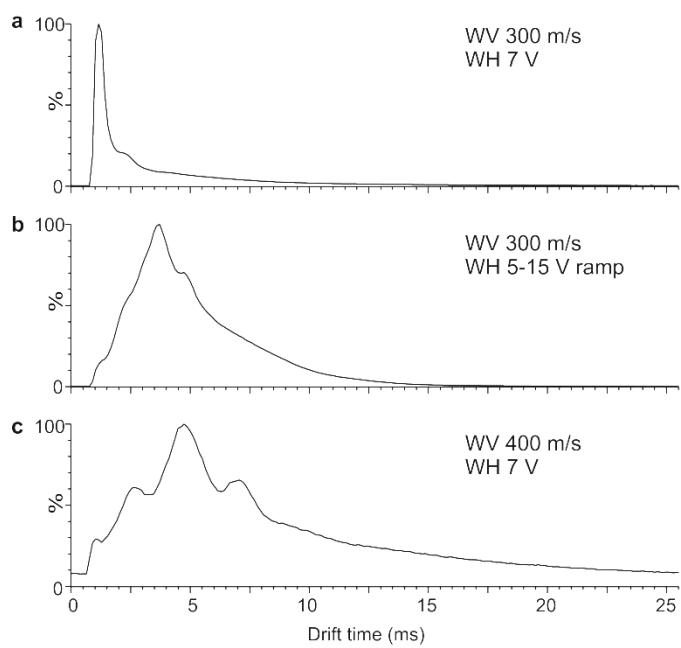
**Tables**

Table 1. Instrument parameters of importance for protein oligomer analysis

| | |
|---|---|
| **Backing Pressure** | 3-7 mbar |
| **Capillary voltage** | 0.8-1.7 kV |
| **Sample cone** | 20-170 V, above approximately 60 V monomeric protein may be activated and start to unfold yet higher-order oligomers may only be observed at higher cone voltage |
| **Extraction cone** | 0-10 V, again if this is too high monomer may be activated but at low values oligomeric species may not be transferred into the instrument effectively |
| **Trap collision energy** | 6-40 V, higher values will improve mass accuracy but may induce gas-phase unfolding/dissociation |
| **Transfer collision energy** | 4-40 V, at higher voltages dissociation/unfolding may occur but transmission of higher-order species may be improved |
| **Trap/transfer pressure** | 0.01-0.05 mbar (Ar) |
| **Ion mobility pressure** | 0.5 mbar ($N_2$) |
| **Ion mobility mode** | |
| *Trap DC Entrance* | 3.0 V |
| *Trap DC Bias* | 16-24 V, protein dependent |
| **Tri-Wave IMS** | |
| *Wave height* | 5-25 V |
| *Wave velocity* | 200-400 *m/s* |
| **Quadrupole MS profile** | This should be optimised for the desired mass range |

$$y = 522.45x^{0.4176}$$
$$R^2 = 0.9762$$